

# **The Squamish ProDelta: Monitoring Active Landslides and Turbidity Currents**

**John E. HUGHES CLARKE, Steve BRUCKER, James MUGGAH, Ian CHURCH,  
Doug CARTWRIGHT, Pim KUUS, Travis HAMILTON,  
Danar PRATOMO and Brad EISAN, Canada**

## **SUMMARY**

A 10 month long program of repetitive surveying of the Squamish delta was completed from November 2010 to September 2011. The aim of the program was to monitor temporal change on the delta front as the snowmelt-driven freshet waxed and waned.

93 discrete surveys were performed at time scales ranging from monthly (in the winter) to daily (in the summer). Inter-survey changes reveal the onset of significant sediment transport on the delta top channels and mass wasting on the prodelta slope. They also reveal the evolution of the sediment transport character and mass wasting style through the freshet period. Correlations with discharge peaks and tidal range can clearly be seen.

Targets were laid in the path of the mass wasting and a bottom mounted ADCP was installed just seaward of the previously recognized significant change. These in-situ seabed monitoring methods clearly indicated bulk displacement of the seabed on the upper prodelta slope and full development of turbidity currents on the lower prodelta slope. Water column sections along the active sediment pathways were conducted every weekday throughout the summer, often revealing clear disturbance of the deep-scattering-layer in the fjord suggesting deep water mass injection.

Having simultaneous precise surface change maps and in-situ instrumentation provides an unprecedented view of landslide processes in a coastal fjord environment. The Port of Squamish is one of the West Coast's major shipping hubs and, together with the Sand Heads section off Vancouver and the proposed Northern Gateway terminus at Kitimat, are all vulnerable to active submarine landslides.

**Key words:** Submarine Landslides, Turbidity Currents, Multibeam Water Column, Seabed Change Detection.

## **1. INTRODUCTION: HYDROGRAPHIC CHANGE DETECTION**

Coastal infrastructure development needs to account for potential changes in the local submerged geomorphology over time scales of decades. For historical reasons (when the river was the means of access to the interior) ports and harbours are often located at river mouths which themselves tend to be areas of particularly rapidly changing subaerial and submarine relief. Thus hydrographic surveys are normally required to monitor the evolving bathymetry to both ensure

immediate under-keel clearance and monitor the long-term encroachment of shoals on navigational channels.

Analysis of successive hydrographic surveys has long been the key to identifying natural sedimentary processes (e.g. Tizard, 1890). Examining the apparent change through repetitive surveying requires particular attention to be paid to the use of common vertical and horizontal datums. Furthermore systematic biases in each of the compared surveys need to be clearly isolated. In the limit, the uncertainty in the observations limits the resolvable change. The longer the time scale, the easier it normally is to identify change.

Without 100% coverage, any analysis is vulnerable to aliasing issues due to unresolved relief at wavelengths shorter than the sampling interval (traditionally the single beam line spacing). With the advent of near 100% coverage multibeam systems, the spatial density is now sufficient to both monitor long wavelength shoaling and identify short wavelength ephemeral or migrating seabed features. We thus now have the ability to both monitor regional change (without aliasing problems) and potentially identify the active seabed mechanisms that drive that change.

## **2. SURVEY AIMS, DESIGN AND INSTRUMENTATION**

### **2.1 Aims of the Squamish ProDelta Survey**

The specific aim of this survey was to try and resolve the timing, mechanism(s) and result of mass wasting processes that occur on the prodelta of the Squamish Delta in Howe Sound, British Columbia. The Squamish prodelta was first identified as a site of enhanced submarine mass wasting in the early 1980's (Prior and Bornhold, 1984). Biannual, annual and semiannual multibeam surveys have been conducted there since 2004 (Brucker et al. 2007). Those surveys clearly indicated that the morphology of the prodelta is being significantly altered, primarily during the summer freshet period (Hughes Clarke et al., 2009). During that period the river discharge rises from a winter time level of less than  $100\text{m}^3/\text{s}$  to about  $500\text{m}^3/\text{s}$  for about 4 months (Hickin, 1989). Interspersed with the increased flow are local surges of up to  $\sim 1000\text{m}^3/\text{s}$ . (Fig. 1).

The style of the mass wasting controls the long term progradation of the delta and potentially might indicate whether catastrophic collapses are likely to occur. The long term progradation will ultimately limit the viability of the current Squamish Terminal infrastructure. The possibility of catastrophic collapse is a potential tsunami hazard that could affect both the port and the town. A comparable situation is known to exist for the Sands Head section of the Frazer Delta (Mosher et al., 1997) and has previously generated catastrophic results for the case of the Kitimat Delta (Murty, 1979). The Sands Head prodelta slope is currently undergoing an analogous program of multibeam resurveys (Hill, 2012). The 6-7m high tsunamis at Kitimat in October 1974 and April 1975 are known to have been triggered by submarine landslides (Prior et al. 1982) and are currently being reassessed as a potential geohazard affecting the proposed development of the Northern Gateway Terminal (AMEC, 2011).

While fjord delta mass wasting is a process of particular significance to the Canadian West Coast, more generally, submarine mass wasting is an imperfectly understood process. Analogous deep ocean events are only rarely observed (e.g. Heezen and Ewing, 1952, Hsu et al., 2008) and

incomplete knowledge normally exists of the state of the seafloor before the event so the change cannot be directly measured. As a result, the majority of inferences about the mechanisms for deep ocean mass wasting are gleaned from the sedimentary or rock record and through analogy with laboratory scale experiments (e.g.: Hampton, 1972, Mohrig et al., 1998). Thus any opportunity to examine modern active mass wasting in which the state of the seafloor before and immediately after can be compared, is of great interest. The fjord head deltas in BC have previously been shown to generate frequent (10's per year) turbidity currents (Prior et al., 1987, Bornhold et al., 1994) and are thus ideal laboratories to investigate processes analogous to the deep sea.

## 2.2 Survey Design

The survey was designed to try to identify the timing and style of mass wasting events on the prodelta slope during the summer freshet period. To that end, repetitive multibeam surveying was utilized with an interval that reflects the likely event periodicity. During the winter inactive period, monthly surveys were utilized, but with the onset of the freshet, the surveys were conducted on every week day (Fig. 1). A total of 93 resurveys were conducted in all.

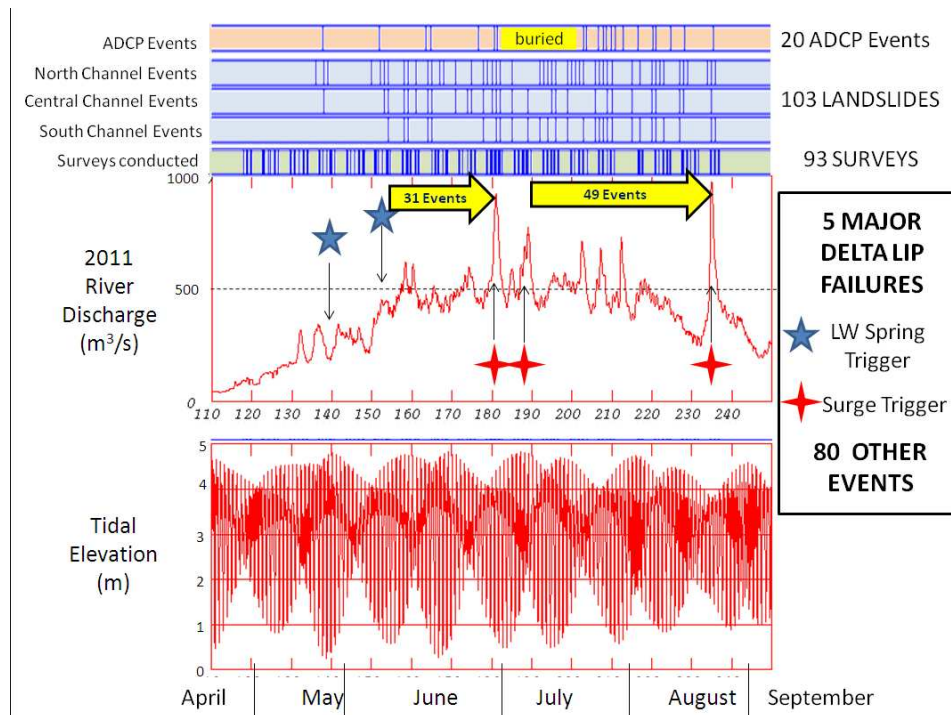


Figure 1: timing of 2011 surveys with respect to the tides and river discharge level

The area covered includes the delta top channel and the prodelta slope extending from the delta lip to water depths of ~200m over a distance of about 3500m (Fig. 2A). On the prodelta slope,

three major active channels are clearly developed (Fig. 2A). Over the whole summer freshet period, all three channels were clearly active (Fig. 2B) and on average, the delta lip regressed. The specific aims of this experiment, however, were to establish when that cumulative surface difference occurred and infer the mechanism for the individual change events. Daily bathymetric difference maps were the prime tool used for identifying the progression of events. For this project, digital terrain models for each epoch (day of survey) were generated and a difference map was derived by subtracting each epoch from the previous one. In this way daily change could be observed as long as it exceeded (or had a distinct pattern with respect to) the apparent change due to systematic biases in one or both of the epoch surveys.

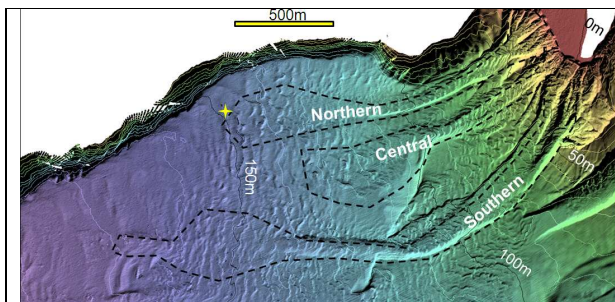


Fig. 2A: Survey area illustrating the three major channels and depth ranges covered. 10m contours in white. Yellow star indicates location of ADCP.

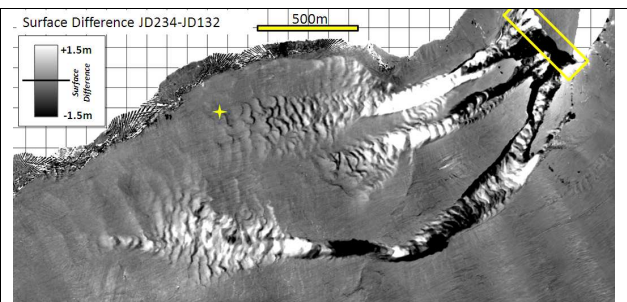


Fig. 2B: Cumulative differences over summer freshet from April to August. Yellow rectangle indicates area of detailed study presented in Figure 3.

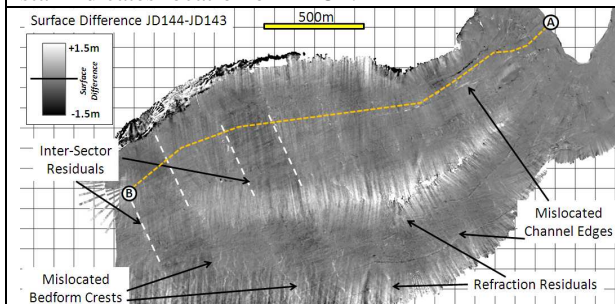


Fig. 2C: Difference map generated from surveys one day apart when no mass wasting was present. This example illustrates the character of the systematic biases present in the two surveys that limit the detection of actual events. A-B represents section shown in figure 5A.

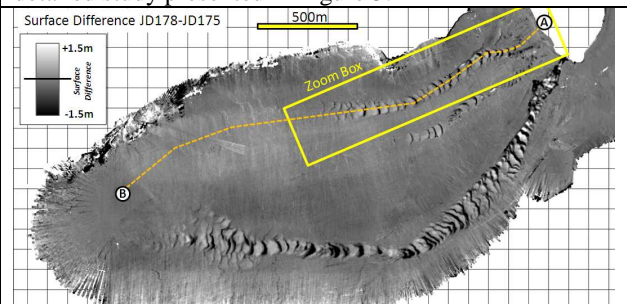


Fig. 2D : Difference map generated from surveys three days apart when active mass wasting was clearly identified in all three of the prodelta channels. Yellow rectangle indicates area of detailed study presented in Figure 4. A-B represents section shown in figure 5B.

Ideally, in the absence of any mass wasting event, there should be no difference between subsequent surveys. Figure 2C presents an example for such a day. As can be seen, the surface differences are within about  $\pm 0.5\text{m}$  (which for depths in the 100-200m range are comfortably within IHO Special Order standards). However, the distribution of apparent change is clearly not random but reflects the projection of systematic biases along the survey swath orientation used. Long wavelength bias patterns are seen reflecting slowly changing biases such as refraction residuals and inter-sector biases. As the orientation of these patterns follows the survey plan

rather than trends in natural geomorphology, they are usual obvious (Fig. 2C). In addition, however, and more confusing to interpretation, are the presence of short wavelength apparent change that result from biases in horizontal positioning that generate errors wherever rapid slope changes take place. The most common location for these to show up are on channel edges and edges of bedforms (Fig. 2C). Such narrow lines of apparent change can easily be confused with natural changes to channel edges or real bedform migration.

When real mass wasting occurs, the most common pattern seen in the difference maps (Fig. 2D) is a reflection of real translation of within-channel bedforms. In the example shown, three discrete mass wasting events occurred within the same 72 hour period, but in separate channels. Note that they are sourced from separate locations at differing depths on the prodelta and their longitudinal extent varies significantly indicating different run-out distances. In all, based on the surveys conducted, a total of 103 discrete seafloor mass wasting events were identified over the summer freshet period.

### 2.3 Instrumentation

The main instrument used was an EM710 multibeam sonar system. It provided both bathymetry, backscatter, and in the case of this project, most innovatively, water column imaging. The accuracy and resolution at which seabed change may be detected is a combination of the capabilities of the sonar itself as well as the associated integrated instrumentation (Hughes Clarke, 2012). For many applications it is the integration itself (inter-sensor alignments, offset and timing), rather than the accuracy of the component sensors that control the resolvable limits of seabed change detection.

#### 2.3.1 Multibeam Bathymetry

The multibeam resolution controls the ultimate achievable limit on accuracy in both horizontal and vertical. The EM710 used has a 1° transmit and a 2° receive beam width. Typical along-track projected beam footprints were thus 2-4% of depth. Across track, through the use of high definition beam forming, discrimination at wavelengths shorter than the projected receiver beamwidth is possible. As a result, 200 bottom detection solutions are generated across-track which are roll stabilized and equidistant spaced. Using multiple transmit sectors, pitch and yaw stabilization is also implemented ensuring an even along track spacing.

The multibeam was operated typically with a 4x water depth sector at 8 knots using dual swath, and with 100% overlap between lines. This resulted in a solution spacing on the seafloor of about 1% of depth (~ 4 x denser than the beam footprint). Data were gridded using a weighted filter with an interpolation radius reflecting twice the beam footprint and thus typically the gridded surface has a ~16x averaging that acts as a spatial filter. As a result of this spatial filtering the incoherent random noise associated with the bottom detection (typically at the 0.1% of depth level ( $1\sigma$ )) was minimized leaving only the coherent systematic biases in the data as artefacts in the gridded surfaces. The nature of those systematic artefacts is the limiting factor in controlling the smallest scale of detectable seabed change.

The two most notable systematic artefacts in the data were found to be refraction residuals and inter sector depth offsets (Fig. 2C). The refraction residuals develop nonlinearly as a function of incidence angle. As most of the surveys were conducted using 200% coverage and with a

weighted filter that is biased toward the lower incidence angles, the refraction residuals only show up where swath edges are exposed. The sector boundary offsets are only intermittently developed which suggest that they might be a result of imperfect surface sound speed assumptions (affecting the transmit steering).

### 2.3.2 Multibeam Backscatter

The EM710 generates an image of bottom backscatter strength estimates across the swath. As with the bathymetry, two swaths are generated using 3 sectors each. The backscatter strength estimates are reduced according to standard assumptions (Hammerstad, 2000). The most significant is the use of a time varying gain that is based on the minimum slant range and assumes a flat seafloor. This flat seafloor assumption can be backed out of the data in post-processing by estimating the local seabed-relative grazing angle (Brucker et al., 2007) which removes much of the local seafloor slope-related backscatter modulations, leaving primarily the backscatter variability due to substrate.

A second limitation is notable sector-specific beam pattern residuals in the data. To remove these, each sector (6 unique sectors per depth mode and three modes used over the depth range seen) have to be isolated and the average signal stacked by elevation angle (Teng, 2012). An additional limitation on the absolute backscatter strength estimates is proper reduction for environmental controls on the attenuation coefficient. Distinguishing whether apparent seasonal variations in the bottom backscatter strength are due to the environment or substrate alteration is a research topic of a parallel paper in this conference (Carvalho and Hughes Clarke, 2012).

### 2.3.3 Multibeam Water Column Imaging

The EM710 logs a down-sampled time series of backscatter along each physical beam forming channel (128 for a 2° receiver used herein). Hay et al., (1982) had previously illustrated that acoustic volume scattering, using a 200 kHz single beam echo sounder, is capable of identifying actively flowing turbidity currents. In that case however, enhanced volume and point target scattering was associated with such flows. In contrast, for the ~80 kHz volume scattering utilized herein, the anomalous bottom following displacements were best characterized by a local drop in the acoustic volume scattering. It is believed that this is associated with displacement of the zooplankton rich (usually euphausids) deep-scattering layer (Hughes Clarke et al., 2012).

### 2.3.4 Horizontal Positioning

If just long wavelength change is desired, then corresponding positioning accuracy need only match and exceed that minimum wavelength. In this case we are interested in the displacement of dune bedforms with typical amplitudes of 5m and wavelength of 40m that have local lee slopes of up to 45°. With such slopes, any horizontal positioning bias will show up as a corresponding apparent depth change (Hughes Clarke et al., 2011). Thus distinguishing real bedform migration from horizontal positioning biases is limited to the achievable horizontal positioning accuracy. For real-time operations, a pseudo differential correction was applied to the POS/MV inertially smoothed GPS solution from a C-Nav receiver. This appears to be capable of providing solutions within 0.5m ( $2\sigma$ , Hughes Clarke et al., 2011). Alternately the raw C-Nav RTG solution could have been used with higher accuracy (~0.25m,  $2\sigma$ ) but with occasional jumps due to poor satellite geometry and intermittent interruptions in the satellite-based correction due to extreme

fjord topography masking satellite visibility.

In post processing we are currently reprocessing all the original pseudo-range data to provide PPP and PPK solutions which generally achieve horizontal positioning confidence in the 0.05 to 0.1m range (at  $2\sigma$ ).

#### 2.3.5 Vertical Positioning

In real time, a predicted tide was utilized. Subsequently the observed tide at Point Atkinson has been obtained. Preliminary analysis suggests that the predicted and observed are within ~ 9cm ( $1\sigma$ ). Long period heave drifting was not a significant factor in these survey operations due to slow speeds. As the PPP or PPK solutions are calculated, the option of replacing the conventional tide-referenced vertical positioning with an Ellipsoid Referenced solution is being investigated.

#### 2.3.6 Oceanographic Measurements

The primary input of sediment to the delta is suspended sediment in the river discharge. Thus an understanding is required of the estuarine circulation of the delta mouth and the plume that extends out into the Howe Sound fjord. Additionally, for the purpose of bathymetric accuracy, the natural variability in the sound speed needs to be adequately captured. Due to the extreme variability in sound speed associated with the freshwater-driven river plume (Hughes Clarke et al., 2011) a combination of rapidly cycling near surface (to 30m) profiling was done using an MVP-30 probe, extrapolated using an statically lowered AML SV and T probe to categorize the much more stable deeper water masses. The MVP had both a CTD for sound speed and an optical backscatter sensor for direct measurement of suspended sediments.

#### 2.3.7 Passive Targets

Based on previous unsuccessful attempts to measure currents directly in canyons (Inman et al, 1976), a method similar to that developed by Paull et al. (2010) was employed. They embedded heavy concrete monuments in the canyon floor sediments, instrumented with an acoustic beacon for tracking. To replicate this experiment without the use of acoustic transponders, heavy seabed markers (2 or 3 breeze blocks) were dropped on the channel floor marked with suspended air filled 6-8 inch diameter spheres. Each target has three sphere suspended above it using unique spacing to allow unambiguous tracking using the EM710 water column imaging. Automated target recognition software (Marques and Hughes Clarke, 2012, this volume) is being developed to identify and locate these targets as they were displaced over the summer freshet period.

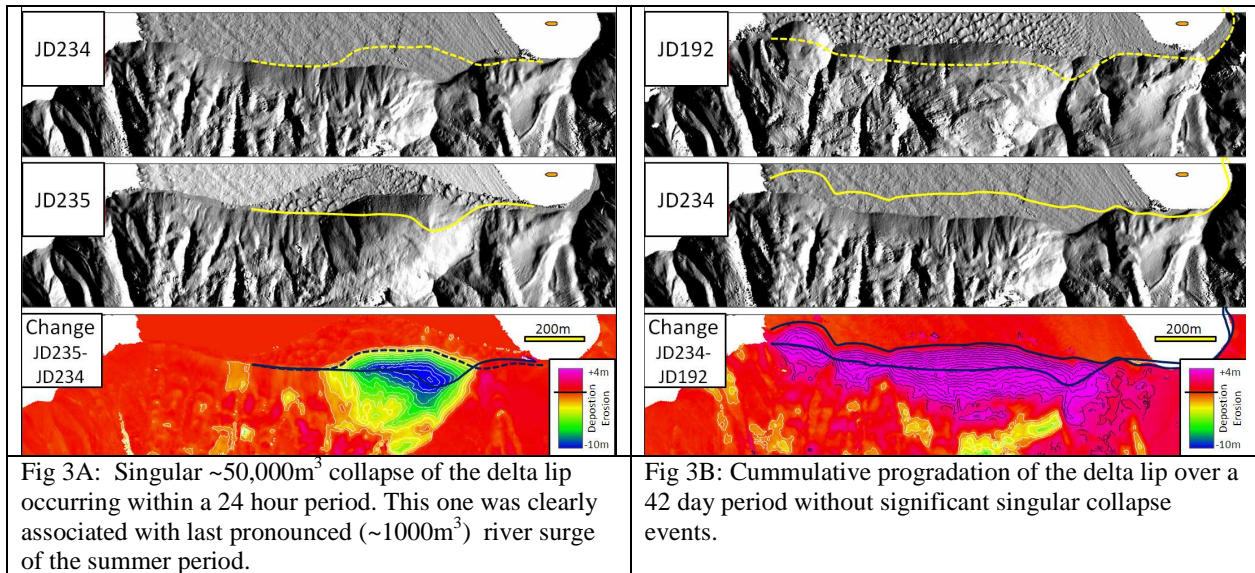
#### 2.3.8 Bottom Mounted Current Meter

Ultimately, direct measurement of near- seabed currents is required to positively identify the active presence of turbidity currents. Measurements of this phenomena are rare (Prior et al., 1987, Khripounoff et al., 2003, Xu et al., 2004). In this study a 600 kHz ADCP was installed in a bottom-mounted tripod in 150m of water just seaward of the termination of the North Channel (Fig. 2A). The ADCP sampled 17 ping ensembles every 30 seconds using 50cm bins up to a maximum elevation of 47m off the seabed. It was recovered every 2 weeks to download the data. It operated continuously throughout the freshet period with the single exception of a 20 day period when it was buried by a mass flow event.

### **3. OBSERVED ACTIVITY AND DAILY CHANGES**

### 3.1 Delta Lip Progradation and Collapse

On every week day, the lip of the delta was surveyed to monitor its progradation and occasional collapse. This break point is particularly sharp and lies within 1m of chart datum. The peak slopes developed here were normally in excess of 40°, well beyond the stable angle of repose of the fine sand sediments.



Once the river discharge exceeded ~ 300 m<sup>3</sup>/s, the delta top subtidal channel clearly exhibited actively migrating bedforms and the MVP optical backscatter indicated high (>0.07g/l) suspended sediment loads. This sediment flux resulted in measurable progradation of the delta lip, interspersed with discrete collapse events. Figure 3A illustrates one of the 5 most noticeable collapse events (ranging from 20 to 150,000m<sup>3</sup>). The first two collapses (Fig 1) were clearly associated with low water spring tides. The subsequent 3 events were associated with abrupt river surges (Fig. 1). Using cumulative lip progradation between major lip collapse events (Fig 3B), preliminary sediment fluxes of about 2-3000m<sup>3</sup> per day were estimated.

### 3.2 Within Channel Bedform Development and Migration

On every week day, the upper 0-50m section of the delta front was surveyed and three sections were run along the three active channels. The aim of these surveys was to try to resolve the periodic migration of channel floor bedforms and occasional larger discrete slide scar and deposit events. Figure 4 illustrates the analysis of one week of daily differences during the most active period. On every day an event had happened and on the last day, the largest event of the year in the North Channel occurred, resulting in a plug of sediment filling the channel talweg, subsequently diverting the sediment out to the side. It was this event that buried the ADCP (located just seaward of the zoom area in figure 4A).

While the channel floor bedform migration is very similar for the first 4 days of the sequence in

Fig. 4A, the upslope and downslope character vary markedly. For JD178-175, the bedform migration extends out beyond the channeled section onto the unconstrained proximal lobe even though the upslope character reveals only minor disturbances on the delta lip. By JD180-179, the change in the delta lip is more evident suggesting more failed sediment available, even though the distal extent of bedform migration is actually reduced. The JD181-180 change constitutes the single largest collapse of the delta lip for the whole summer ( $-150,000\text{m}^3$ ), yet initially that sediment does not appear to have travelled further than the upper channel. But by the following day, that volume is now emplaced as a 4-5m thick plug (Fig. 4B lower) in the lower channelized section completely filling the channel from bank to bank as a positive feature, diverting subsequent flow for the rest of the summer. Bedforms downhill of the plug suggest that the emplacement was preceded by high velocity flow that extended out onto the proximal lobe. It was this event that was briefly detected as a turbidity current by the ADCP before it was completely buried.

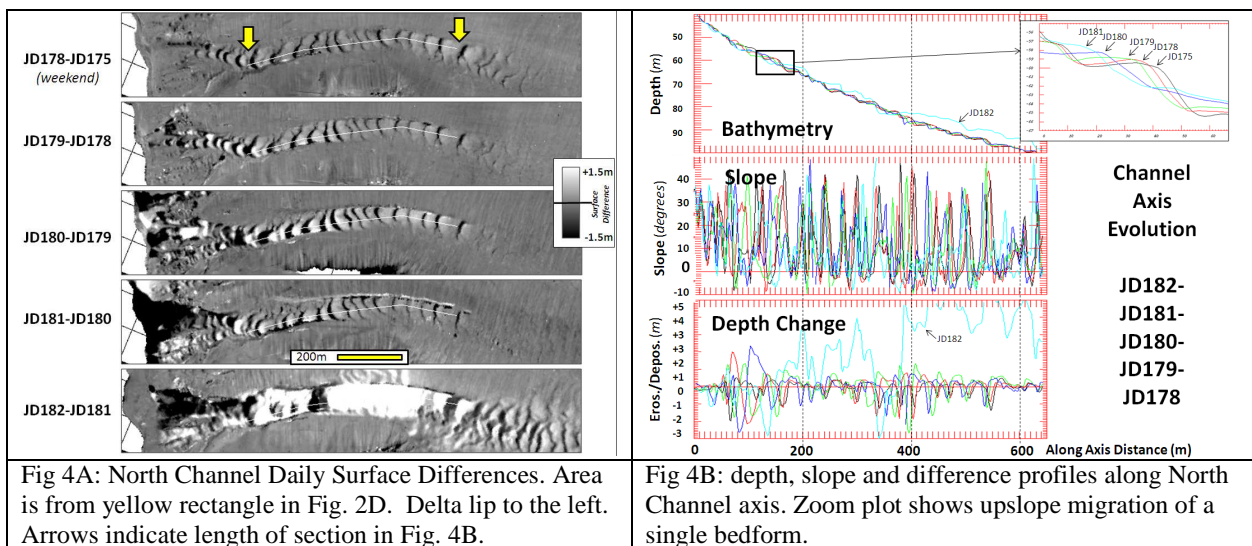


Fig 4A: North Channel Daily Surface Differences. Area is from yellow rectangle in Fig. 2D. Delta lip to the left. Arrows indicate length of section in Fig. 4B.

Fig 4B: depth, slope and difference profiles along North Channel axis. Zoom plot shows upslope migration of a single bedform.

Successive daily sections along the channel clearly indicate unambiguous upslope migration of the periodic bedforms (Fig. 4B, top). The 30-40m wavelength bedforms have downhill facing lee slopes of over  $40^\circ$  and uphill facing stoss sides of up to  $-10^\circ$  (Fig. 4B centre plot). These fluctuations are superimposed on an average channel slope of  $6^\circ$ . In morphology and migration character they most closely resemble the downslope asymmetric non-aggrading cyclic steps described by Cartigny et al. (2011).

### 3.3 Seabed target displacements,

The seabed targets, installed in the channel floors prior to the onset of the freshet, were intended to provide evidence of bulk displacement of the channel floor sediments. The basal blocks are too large to be moved as bedload sediment transport by any of the observed current velocities.

Should, however, the seabed move on mass, either as a grain or debris flow (Paull et al., 2010), then the targets should be displaced along with this. While analysis is incomplete at this time, in-field measurements indicate several 100 metres of displacement of these targets before they appeared to disappear.

### 3.4 Proximal Lobe Bedforms

In addition to the channels, the proximal lobe from the channel mouths to the 200m contour was also surveyed daily. The aim was to try and resolve both bedform migration in the flow expansion area but more particularly to see whether net regional accretion or deflation of the more bedform free areas could be detected.

Bedform migration is limited primarily by the horizontal positioning uncertainty and thus it is relatively clear when active migration was happening. Only a subset of the events examined extended out onto the unconstrained lobe. Bedform displacement generally decreases with distance from the channel mouth suggesting decelerating flow.

What is harder to establish is whether there is a thin (<50cm) blanket of deposition in this region due to a waning flow (that might be insufficiently powerful to resolvably translate the bedforms). In this case, as the deposition is over long wavelengths (100m+) the limiting factor is uncertainty in the vertical component of depth estimation. This is dominated by biases due to tides, sector offsets and refraction uncertainty (Fig. 2C) which are clearly survey line geometry driven rather than related to a real sedimentary process.

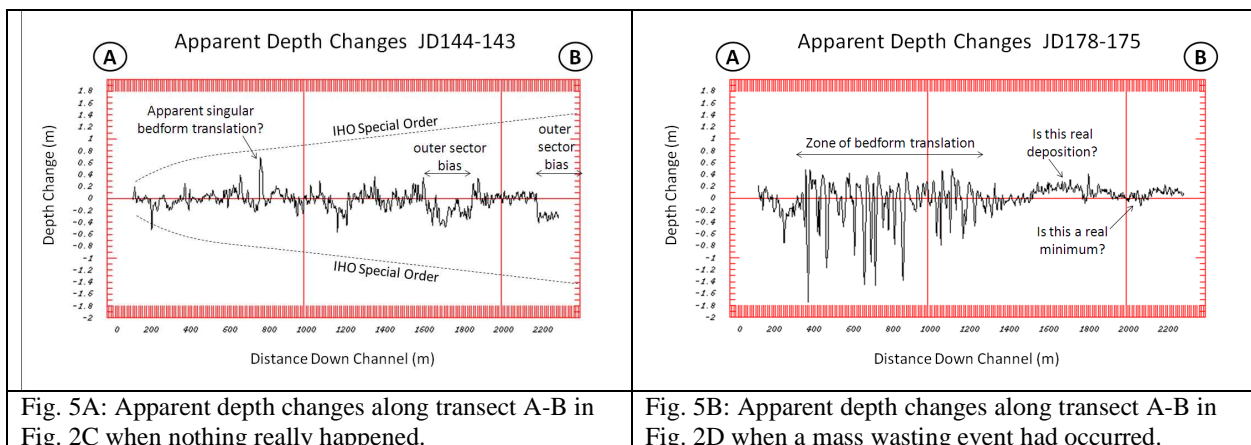


Fig. 5A: Apparent depth changes along transect A-B in Fig. 2C when nothing really happened.

Fig. 5B: Apparent depth changes along transect A-B in Fig. 2D when a mass wasting event had occurred.

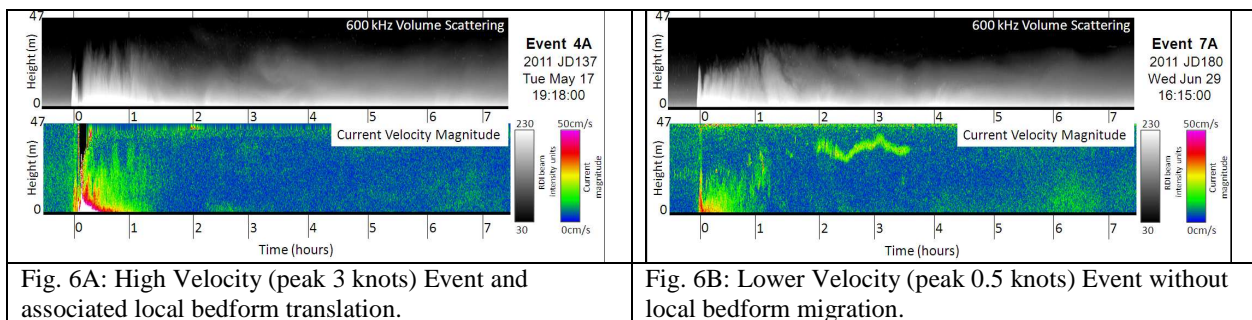
Cross sections through the difference maps in Fig. 2C and D are presented in Fig 5A and B. When nothing really happened (Fig. 5A), there are step-like offsets of about 20cm due to the inter-sector biases. Note that all these residual errors are a very small fraction of the allowable uncertainty for IHO Special Order. When one then cuts a section through the difference map when something did happen (Fig. 5B), while one can clearly see the evidence of the bedform migration (+/-0.5 to 1.5m in this case), the slowly varying apparent change over the several hundred metres seaward of the last dunes cannot be confidently used as evidence for regional

deposition.

Current post-processing of the vertical solution through PPP or PPK and reprocessing of the ray trace may minimize this. However, it is clear that such depositional patterns are at the limit of robust resolvability.

### 3.5 Accompanying ADCP observations

As well as change within the channels and on the proximal lobe, the morphology of the distal basin clearly indicate that sediment transport must occasionally extend into deeper water. The ADCP deployment was designed to catch those events emanating from the Northern Channel. Despite having 48 clear bathymetric change events in that channel, only 20 turbidity current events were detected (Fig. 1). For those events, a rapid (0.5 knots or greater) surge current was developed (Fig. 6) with a duration of over one hour that were transporting suspended sediment (as indicated by the 600 kHz volume scattering). The flow thicknesses ranged from 10 to 40m and the suspended plume was seen to taken more than 8 hours to decay away. While attempts have been made to estimate suspended load concentrations in plumes from ADCP acoustic volume backscatter (e.g.: Hosseini, et al., 2006) these generally assume low density currents so that the particle attenuation is not significant. In this case, the head of the plume is clearly so dense that it masks scattering from higher in the water column.



### 3.6 Water Column Imaging of Displacing underflows

A serendipitous result of the survey design, was acquisition of vertical sections of water column imaging along each of the channel axes that clearly showed events when the deep scattering layer was perturbed by seabed-following underflows (Fig. 7A). By lowering the optical backscatter probe through representative locations in these sections, it is clear that these underflows are water masses of enhanced suspended sediment concentrations (Fig. 7B).

To try and understand whether these events represents an active flow or the “wake” of a flow that has already passed, the character of active gas plumes was utilized (Fig. 7B). The prodelta was found to have a high density of active gas plumes that were clearly imaged in the water column acoustic volume scattering. While no physical samples of these plumes have been recovered to date, assuming typical bubble populations, ascent rates should be of the order of ~ 10cm/s. Thus a plume in a stagnant body of water would be expected to rise vertically. But if it were rising through a moving body of water it should be laterally translated. Figure 7B illustrates the tilt that

should be observed for bubble plumes for a variety of current speeds. As can be seen, in the example illustrated, the bubble plumes are nearly vertical indicating that while the zooplankton remain displaced, the water mass was not moving within several minutes of the imaging period.

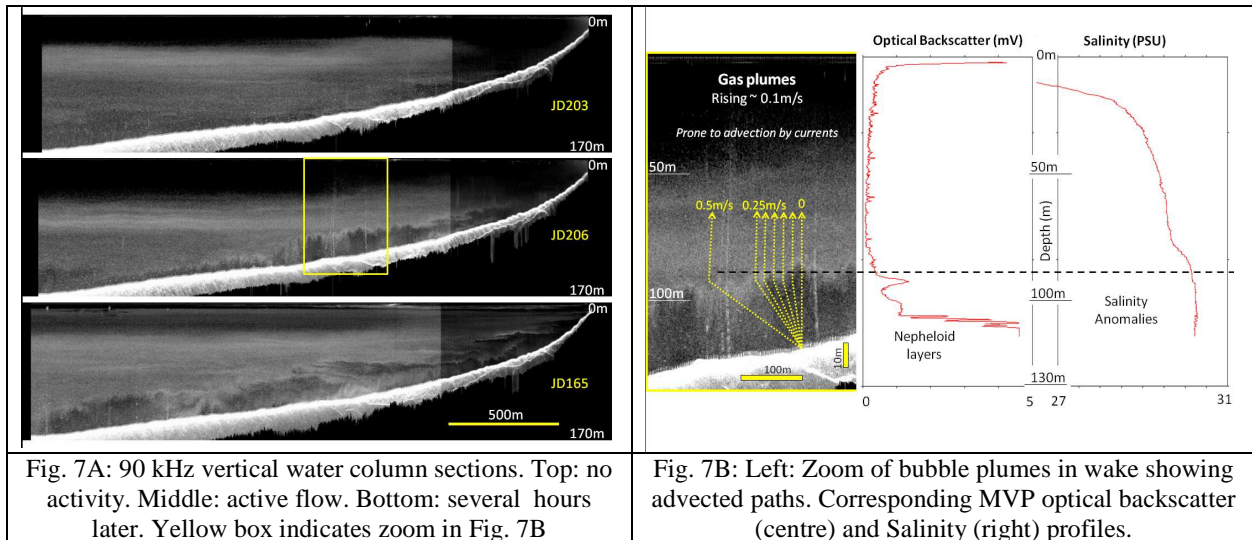


Fig. 7A: 90 kHz vertical water column sections. Top: no activity. Middle: active flow. Bottom: several hours later. Yellow box indicates zoom in Fig. 7B

Fig. 7B: Left: Zoom of bubble plumes in wake showing advected paths. Corresponding MVP optical backscatter (centre) and Salinity (right) profiles.

### 3.7 Distal Lobe Backscatter

Every two weeks, the full distal basin, from the 200m contour to the Porteau Cove Sill was surveyed. At these depths, annual accumulation rates are estimated to be 5-10cm/yr at the 200m contour and less than 0.2mm a year at the 285m deep ponded basin (Hickin, 1989, Fig 2, Equation 1). Such changes are thus unlikely to be resolvable through surface bathymetric methods. Nevertheless, previous surveys (Hughes Clarke et al., 2011) had illustrated that the magnitude and angular response of the backscatter could appear markedly different from winter to summer. This might suggest changes in surface roughness over that period, perhaps linked to the laying down of turbiditic layer(s) and their subsequent bioturbation.

The two-weekly distal survey may reveal this character. At this time however, a major focus is on ensuring that the deep backscatter data is appropriately corrected for changing environmental issues over the year as the water mass attenuation changes significantly with temperature (Carvalho and Hughes Clarke, 2012) obscuring any real change.

## 4. CONCLUSIONS AND REMAINING QUESTIONS

The timing, scale and style of mass wasting on the Squamish Prodelta slope has been monitored over the 2011 summer freshet period. 103 discrete mass wasting events, consisting of trains of displacements along one of the three active channels, were identified. Five of those events are clearly triggered by a major (> 20,000 m<sup>3</sup>) collapse of the delta lip. The first two of those collapses occurred before the main freshet and are clearly associated with low water springs, strongly suggesting that the triggering mechanism was a local decrease in relative pore pressure.

The later three events were not associated with a low water spring but were clearly correlated with peaks in the river discharge (surging to  $> 800\text{m}^3/\text{s}$  from  $\sim 400\text{m}^3/\text{s}$ ).

While the major collapses provide clear source locations for the train of displaced sediment, the associated down channel displacements were often on the same scale as many of the other 80+ events that are not associated with such major delta lip collapses. Thus an alternate initiating mechanism still remains to be well described.

The trains of successive deposition and erosion associated with the periodic bedforms in the channel floor are clearly seen to be a result of upslope migration. Their morphology closely resembles the cyclic steps (Cartigny et al. 2011) that are currently being used as a model for reinterpretation of many deep sea bedforms believed to be associated with mass wasting. Such a mechanism requires an overriding stream of flowing suspended sediment that alternately is supercritical on the lee faces of the steps (thus erosional) and subcritical on the stoss faces (thus depositional).

If this is truly the mechanism then a sustained flow would be required rather than a single slide.

The fact that some of the longest trains of bedforms are clearly not associated with significant delta lip or upper prodelta slope slumps suggests an alternate source of sustained suspended sediment supply. One possibility is the production of hyperpycnal flow derived from the active river plume either directly (Mulder and Syvitski, 1995) or indirectly (Parsons et al., 2001).

As bedform migration intermittently extended out onto the proximal lobe, this would suggest that fast flowing suspended sediment is also moving there. The ADCP observations confirm this.

Thus a percentage of the displaced volume must have moved passed these proximal terminal lobes and distributed out on the more distal prodelta. Due to limitations in the total propagated uncertainty in the integrated sonar systems, the fate of sediments transported onto the proximal and distal lobes of the delta cannot be addressed.

## ACKNOWLEDGEMENTS

The work was funded through an NSERC Discovery Grant to the first author (“Precise Seabed Change Monitoring”) as well as sponsorship of the Research Chair in Ocean Mapping at UNB. Current sponsors include: the U.S. Geological Survey, Kongsberg Maritime and Rijkswaterstaat. The success of the field component of the Squamish Prodelta program was, to a large degree, a result of the skill and patience of Gordon Allison.

## REFERENCES

- AMEC, 2011, Landslide-Generated Wave Hazard Analysis, Kitimat Arm, Enbridge Northern Gateway Project: Contract report submitted to Northern Gateway Pipelines Inc., by AMEC Environment & Infrastructure, EG0926008, 39pp.
- Bornhold, B.D., Ren, P. and Prior, D.B., 1994. High-frequency turbidity currents in British Columbia fjords. *GeoMar. Lett.*, 14: 238-243.
- Brucker, S., Hughes Clarke, J.E., Beaudoin, J., Lessels, C., Czotter, K., Loschiavo, R., Iwanowska, K. and Hill, P. 2007, Monitoring flood-related change in bathymetry and sediment distribution over the Squamish Delta, Howe Sound, British Columbia: U.S. Hydro. Conf. 2007, 16pp.

- Cartigny, M.J.B., Postma, G., van der Berg, J.H. and Mastbergen, D.R., 2011, A comparative study of sediment waves and cyclic steps based on geometries, internal structures and numerical modeling: *Marine Geology*, Volume 280, Issues 1–4, 15 February 2011, Pages 40-56.
- Carvalho R. and Hughes Clarke, J.E., 2012, Proper environmental reduction for attenuation for multi-sectors sonars: CHC 2012, this volume.
- Hampton, M.A., 1972, The Role of Subaqueous Debris Flow in Generating Turbidity Currents: *Journal of Sedimentary Research*, V. 42, p. 775–793.
- Hammerstad, E. (2000). "EM Technical Note: Backscattering and Seabed Image Reflectivity": Kongsberg Technical Documentation.
- Hay, A.E., R. W. Burling, J. W. Murray, 1982, Remote Acoustic Detection of a Turbidity Current: *Science*, New Series, Vol. 217, No. 4562, pp. 833-835.
- Heezen, B.C. and Ewing, M., 1952. Turbidity currents and submarine slumps, and the 1929 Grand Banks earthquake: *Am. Jour. Sci.*, 250: 849-873.
- Hickin, E.J., 1989, Contemporary Squamish River sediment flux to Howe Sound, British Columbia: *Canadian Journal of Earth Sciences*, v.26, p.1953-1963.
- Hill, P., 2012, Changes in submarine channel morphology and slope sedimentation patterns from repeat multibeam surveys in the Fraser River delta, western Canada, *International Association of Sedimentologists, Special Publication #44.*, Part 1, p.47-70.
- Hosseini, S.A., Shamsai, A., and Ataie-Ashtiani, B., 2006, Synchronous measurements of the velocity and concentration in low density turbidity currents using an Acoustic Doppler Velocimeter: *Flow Measurement and Instrumentation*, v. 17, no. 1, p. 59–68, doi: 10.1016/j.flowmeasinst.2005.05.002.
- Hsu S.K., J. Kuo, C-L. Lo, C-H. Tsai, W-B. Doo, C-Y. Ku and J-C. Sibuet, 2008, Turbidity Currents, Submarine Landslides and the 2006 Pingtung Earthquake off SW Taiwan: *Terr. Atmos. Ocean. Sci.*, Vol. 19, No. 6, 767-772.
- Hughes Clarke, J.E., S. Brucker, J. Muggah, T. Hamilton, D. Cartwright, I. Church and P. Kuus, 2012, Temporal progression and spatial extent of mass wasting events on the Squamish prodelta slope: 11th International Symposium on Landslides, Banff, June 2012, Conference Proceedings, 6pp.
- Hughes Clarke, J.E., Brucker, S., Hill, P. and Conway, K., 2009, Monitoring morphological evolution of fjord deltas in temperate and Arctic regions: *International Conference on Seafloor mapping for Geohazard Assessment*, Editors: Chiocci F. L., Ridente D., Casalbore D., Bosman A, Società Geologica Italiana, Vol. 7, part 4, p.147-150.
- Hughes Clarke, J.E., 2012, Optimal use of multibeam technology in the study of shelf morphodynamics: *International Association of Sedimentologists, Special Publication # 44, Sediments, Morphology and Sedimentary Processes on Continental Shelves: Advances in technologies, research and applications*, Part 1, p. 1-28.
- Hughes Clarke, J.E., Brucker, S., Muggah, Ian Church, I. and Cartwright, D., 2011, The Squamish Delta Repetitive Survey Program: A simultaneous investigation of prodeltaic sedimentation and integrated system accuracy : *U.S. Hydrographic Conference 2011. Proceedings*, <http://thsoa.org/us11papers.htm>, 16pp.
- Inman, D. L., C. E. Nordstrom, and E. F. Reinhard, 1976, Currents in submarine canyons: An air-sea-land interaction, *Annual Rev. Fluid Mech.*, 8, 275– 310.
- Khripounoff, A., A. Vangriesheim, N. Babonneau, P. Crassous, B. Dennielou and B. Savoye, 2003, Direct observation of intense turbidity current activity in the Zaire submarine valley at 4000 m water depth : *Marine Geology*, v.194(3-4) : p.151-158.
- Marques, C.R. and Hughes Clarke, J.E. 2012, Automatic Mid-Water Target Tracking using Multibeam Water Column: CHC 2012, this volume.
- Mohrig, D., Ellis, C., Parker, G., Whipple, K.X. and Hondzo, M., 1998, Hydroplaning of subaqueous debris flows : *Geological Society of America Bulletin*, March, 1998, v. 110, no. 3, p. 387-394
- Mosher, D.C, J.A. Hunter, H.A., Christian, and J.L. Luternauer, 1997. Onshore/offshore geohazards in the Vancouver Island region of western Canada: field, modelling and mapping techniques and results, In: *Marinos, P.G., Koukis, G.C., Tsiambaos, G.C., and Stournaras, G.C. (eds.), Engineering Geology and the Environment*,

- Balkema Publishers, Rotterdam, 875-883.
- Mulder, T. and Syvitski, J.P.M., 1995, Turbidity currents generated at river mouths during exceptional discharges to the world oceans. *Journal of Geology*, v.103, p.285-299.
- Murty, T.S., 1979. Submarine slide-generated water waves in Kitimat Inlet, British Columbia, *Journal of Geophysical Research*, 84(C12), 7777-7779.
- Parsons, J.,D., J.W. M. Bush and J.P. M. Syvitski, 2001, Hyperpycnal plume formation from riverine outflows with small sediment concentrations: *Sedimentology* v. 48, p.465-478
- Paull, C.K., Ussler, W., Caress, D.W., Lundsten, E., Covault, J.A., Maier, K.L., Xu, J., and Augenstein, S., 2010, Origins of large crescent-shaped bedforms within the axial channel of Monterey Canyon, offshore California: *Geosphere* (December 2010), 6(6):755-774.
- Prior, D.B., B.D. Bornhold, J.M. Coleman and W.R. Bryant. 1982. Morphology of a Submarine Slide, Kitimat Arm, British Columbia. *Geology*, Vol. 10, p. 588-592.
- Prior, D.B. and Bornhold, B.D., 1984, Geomorphology of Slope Instability Features, Bathymetry Squamish Harbour, Howe Sound, British Columbia: Geological Survey of Canada, Open File 1095. – 2 Maps. 1-10,000
- Prior, D.B., Bornhold, B.D., Wiseman, W.J, and Lowe, D.R., 1987. Turbidity current activity in a British Columbia fjord. *Science* 237: 1330-1333.
- Teng, Y.T. 2012, Sector-specific Beam Pattern Compensation for Multi-sector and Multi-swath Multibeam Sonars: MscEng thesis, Department of Geodesy and Geomatics Engineering, UNB, 107 pp.
- Tizard, T.H., 1890, The Thames Estuary, *Nature*, v.41, p.539-544.
- Xu, J.P., M. A. Noble and L. K. Rosenfeld, 2004, In-situ measurements of velocity structure within turbidity currents: *Geophysical Research Letters*, v. 31, L09311, doi:10.1029/2004GL019718.

## BIOGRAPHICAL NOTES

**Hughes Clarke** : is a Professor in the Department of Geodesy and Geomatics Engineering (GGE) and the Chair in Ocean Mapping at the University of New Brunswick (UNB).

**Brucker, Muggah, Church, Cartwright and Kuus** : are all graduates of, and Research Assistants within, the Ocean Mapping Group (OMG) at UNB. They design, implement and manage multibeam surveys as part of the OMG and ArcticNet programs. Cartwright now teaches Ocean Mapping at the Marine Institute at Memorial University of Newfoundland.

**Hamilton and Pratomo** : are current graduate students within the OMG at UNB working on marine geomatics issues on the Squamish Delta.

**Eisan** : was a current final year undergraduate student within GGE at UNB. He now works for Fugro Jacques Geosurveys in St. John's NL.

## CONTACTS

John E. Hughes Clarke  
 Dept. Geodesy and Geomatics Engineering, University of New Brunswick  
 P.O. Box 4400, Fredericton, NB, E3B 5A3, CANADA  
 Tel. +1-506-453-4568, Fax +1-506-453-4943  
 Email: [jhc@omg.unb.ca](mailto:jhc@omg.unb.ca)  
 Web site: <http://www.omg.unb.ca/~jhc>